The Scaffold Derived from GGTA1 and CMAH Gene Knockout Pigs Generated by Gene Editing Provoked Little Inflammatory Responses in a Humanized Pig Model

chon-ho yen
Agricultural Technology Research Institute https://orcid.org/0000-0002-5575-557X
Hao-Chih Tai
National Taiwan University Hospital
Su-Hei Peng
Agricultural Technology Research Institute
Tien-Shuh Yang
National I-Lan University
Ching-Fu Tu (cftu@mail.atri.org.tw)
Division of Animal Technology, Animal Technology Laboratories, Agricultural Technology Research Institute

Research

Keywords: SIS-ECM, Gene Knockout, Pigs, α-Gal, N-glycolylneuraminic acid, IL-6

Posted Date: February 11th, 2020

DOI: https://doi.org/10.21203/rs.2.23159/v1

Abstract

Background

The porcine small intestinal submucosa ECM (SIS-ECM) has been used as a supportive scaffold for healing in a variety of tissues. However, the outcomes of its application are far from satisfactory.

Results

The possibility of generating a porcine small intestinal submucosa extracellular matrix (SIS-ECM) that is fully biocompatible was investigated. Samples of SIS-ECM were prepared from either domestic wild-type (WT) or double-gene knockout (dKO) pigs without antigenic responses to α-Gal and N-glycolylneuraminic acid (Neu5Gc). The scaffolds, which were sutured into cuts made in the longissimus muscle of the dKO pigs, were expected to exhibit xeno-reactions through natural antibodies as in a human response. A process was established to manufacture ameliorating acellular porcine SIS-ECM implants with consistent quality characteristics, which were assured by analyzing the level of residual DNA, the glycosaminoglycan content, and histochemical stains. Once implanted, the acellular SIS-ECM from the WT pigs caused a significant increase in serum IL-6 levels in the dKO recipient pigs, indicating a host defense through immune reactions. The levels remained unchanged when preparations from the dKO pigs were used. The pathological score of the multinuclear giant cells of the dKO (WT) group (2.3±0.5) was significantly greater than that of the dKO (dKO) group (0.7±0.3).

Conclusion

The IL-6 levels and pathological evidences suggested that dKO pigs without α-Gal or Neu5Gc antigenic causing lower inflammatory response can serve as biocompatible SIS-ECM donors or as animal models for testing anthropomorphic immune responses to biomedical devices.

Background

The extracellular matrix (ECM) is a noncellular structure required for the process of forming a new networks and tissues and has now become a successful and widely used medical material in various forms. The porcine small intestinal submucosa ECM (SIS-ECM) has been used as a supportive scaffold for healing in a variety of tissues, including arterial and venous tissues, tendons and wound closures [1-4]. The porcine SIS-ECM consists of collagen, proteoglycan glycosaminoglycan, glycoprotein, and growth factors, and it has been approved as a commercial biomaterial for a variety of clinical applications [5,6]. However, the outcomes of its application are far from satisfactory; prominent noninfectious swelling and severe pain at the site of implantation often accompany its use because of the contamination of porcine DNA [7] and the Gal epitope, which both evoke immune responses [8]. In general, matrix decellularization can be achieved by processing efforts; the side effects from using the SIS-ECM in clinical applications is approached based on the consequences of a deleterious innate antigen response.

The α-Gal epitope is the chief antigen responsible for hyperacute rejection in xenotransplantation but there is a further non-Gal antigenicity concern. In vertebrates, glycans usually have terminal sialic acids that function as markers in normal cells and are recognized by a variety of receptors (e.g., siglecs) [9] to mediate intercellular and intracellular communication. However, the sialic acid family includes several derivatives of the nine-carbon sugar neuraminic acid. In pigs, apes, and Old World nonhuman primates, N-glycolylneuraminic acid (Neu5Gc) is the non-Gal antigen primarily expressed but in humans it is N-acetyneuraminic acid (Neu5Ac) [10]. These innate anti-Neu5Gc antibodies inevitably provoke chronic inflammation that chiefly contribute to the side effects from the use of porcine SIS-ECM [11].

Depleting α-Gal and converting Neu5Gc to Neu5Ac of human form to diminish the antigenicity can be achieved only by knocking out the responsible genes in the pig genome. The α-Gal free or GGTA1 knockout (KO) pigs [12] and Neu5Ac (Neu5Gc free) or CMAH KO pigs [13] have already been generated through our continuous efforts with adopted CRISP/Cas9 gene editing techniques. Thus, the humanized porcine (HP) SIS-ECM that can be obtained from the dKO pigs can also serve as an animal model for antigenicity testing. In accordance with these possibilities, this study was designed to investigate and compare the healing process of artificially induced skin wounds dressed with either HP or WT SIS-ECM in dKO pigs that simulate the immune response of human. The allotropic dressing preparations were expected to reveal the innate antigens suspected of causing side effects and enhance the understanding of the advantages of using multigene KOs in more biocompatible scaffolds or to generate tissues.

Materials And Methods

Animals and Animal care

The GGTA1 KO and CMAH KO pigs were generated by Chung et al. [12] and Tu et al. [13], respectively, by CRISPR/Cas9 gene editing. In this study, the animals were generated by cross breeding GGTA1 KO boars with CMAH KO sows. All animals were reared in a station that was free from specific pathogens (atrophic rhinitis, *Mycoplasma hyopneumoniae*, pseudorabies, *Actinobacillus pleuropneumoniae*, swine dysentery, scabies, classical swine fever, foot and mouth disease and porcine reproductive and respiratory syndrome). The pigs receiving the SIS were housed in individual cages of 2 m^2/20 kg pig body weight, under artificially lighting (450-600 lux for 9 h per day) and sunlight through windows. The animals were fed a restricted (4% body weight) commercial diet formulated to meet the requirements recommended by the National Research Council (2012) and had free access to water. The donors were scarified by sedation, electrical stunning and exsanguinated. The porcine jejunums of the WT and KO animals were obtained from the experimental slaughterhouse. The intestines were ligated at each end of the jejunum and the ileum by cotton threads and incised. The jejunums and ileums were procured, placed into an ice-filled container and transferred to a nearby laboratory for further processing. Permission to undertake the SIS implantation experiments was granted by the institution (IACUC Approval Nos. 105129 and 107060, Agriculture Technology Research Institute) where the animal study was conducted.Blood samples were collected from the anterior vena cava of all pigs under restraining at days 1, 2, 5, 7 and 14 of the implantation of the SIS-ECM (day 0) and placed in tubes without additives to prepare serum for

measuring serum IL-6 concentration. The pathologic study tissues were harvested from the sacrificed recipients at week 1, 2 and 4 after implantation.

Preparation of the SIS-EMC

The porcine SIS-EMC was prepared by the procedure including mechanical disassociation, detergent treatment, and sterilization by peracetic acid. The jejunum samples were carefully removed from the excess mesentery tissue and inverted. Then, the samples were thoroughly and repeatedly rinsed by reverse osmosis water to remove debris. The jejunum samples were cut into lengths of approximately 20 cm and frozen at -30℃ before use. The SIS was isolated using a well-established method of preparation [14,15].

The decellularization protocol was performed by immersing the SIS (3×20 cm) in 100 mL 0.2% SDS saline solution for 4 h under room temperature with moderate shaking. After changing to a new SDS solution, a secondary decellularization step was performed under the same conditions for 16 h. The decellularized SIS was removed and then thoroughly rinsed with deionized water, and perfused for around 15 min with deionized water until the water reached pH 7.0. ± 0.5.

The decellularized SIS membrane (80 cm^2) was cut into 2×2 cm sections and placed into sterile tubes with 50 mL of 0.1% peracetic acid (v/v) for 2 h with gentle shaking. After sterilization, the peracetic acid was cleaned from the decellularized SIS membrane by five times flushing with 50 mL of saline. The sterilized, decellularized SIS membrane successfully passed the bioburden test.

DNA Quantification

About 50 mg SIS samples immersed in 400 μL of lysis buffer (20 mM Tris-HCl, pH=8.0; 40 mM EDTA-Na; 80 mM NaCl; and 0.2% SDS) were minced into small pieces with sterile scissors. The tissues were incubated at 56℃ and digested with 20 mg/mL proteinase K until the tissue pieces could no longer be seen in the solution. A total of 900 μL of equilibrated phenol was added, and the solution was mixed gently by inversion for 10 min. The tubes were centrifuged at 13,000×g for 10 min at room temperature. The upper aqueous layer was pipetted to another clean tube. Next, the extraction procedure was conducted with phenol/chloroform (1/1, v/v) and then with chloroform. The upper aqueous DNA solution was mixed with 600 μL of isopropanol and was centrifuged at 13,000×g for 10 min to precipitate the DNA. The DNA pellet was washed with 70% ethanol and then 100% ethanol and dried at 55℃ in an oven. The DNA was quantified using the Qubit® dsDNA HS assay kit (Invitrogen, USA) and measured with the Qubit® fluorometer (Invitrogen, USA).

Nested PCR for detecting porcine DAP 12 DNA

Nested PCR was used to detect the porcine DAP 12 DNA in the SIS-ECM samples [7]. For the first amplification step, a pair of outer primers (forward: 5’-AATGGACTCCTGCCT CTC-3’ and reverse: 5’-CCTGGACAAGGCTGAAAC-3’) was used in the PCR assay and was expected to produce a 426 bp

amplicon. The resulting product from the initial PCR was used as a template for a second set of primers (forward: 5'-AGAAAAGCAAAGGGGTGGGG-3' and reverse: 5'- AAGGGTGGACAGCAAGGTCC-3'). The nested pair of primers was expected to amplify a 223 bp amplicon by PCR. Fifty microliters of the PCR amplification mixture was prepared in a PCR tube containing 5 µL of the target DNA sample and 1 µL of each primer (200 pmol). The DNA was denatured at 94℃ for 2 min and then amplified by 30 cycles with annealing temperature at 54℃. After the amplification, 10 µL from each PCR product solution was loaded onto a 2.0% agarose gel, which was then stained with ClearVision DNA stain (Protect Technology Enterprise Co., Ltd. Taiwan), and then, the products were observed under UV light. Every PCR run included positive (DNA from untreated porcine small intestine) and negative (water) controls.

Glycosaminoglycan content

Transferred 25 mg of SIS samples or bovine collagen, accurately weighed, into a 1.5 mL microcentrifuge tube containing 180 µL of sterile PBS solution and then were minced into small pieces by sterile scissors. Then, 20 µL of a proteinase K solution (600 units /mL) was added to the mixture, and incubated at 56℃ for 15 min and cooled to room temperature. Deionized water was used to dilute the mixture to obtain a concentration of 12.5 mg/mL of each sample. Then, 100 µL of heparin in concentrations based on the standard curve (20 µg/mL, 50 µg/mL, and 100 µg/mL), a blank solution (water), SIS samples, and a collagen control (containing less than 1 µg of glycosaminoglycan per mg) were added to 250 µL of 1,9-dimethylmethylene blue solution (16 mg 1,9-dimethylmethylene blue (Sigma-Aldrich, catalog number: 341088) in 1 L of solution containing 40 mM glycine and 40 mM NaCl, pH 3.0. The solution was mixed on a vortex for 1 sec, and read the absorbance at 525 nm immediately. A standard curve of the absorbance versus the concentration was generated using the average values of each heparin standard solution used and corrected for the blank.

Analysis of the Neu5Gc and Neu5Ac levels by HPLC

Approximately 50 mg samples, including tissues from the ear and/or tail and the small intestine, cut into small pieces in deionized water and then incubated at 95℃ for 30 min. After cooling the samples to room temperature, 0.5 M H_2SO_4 was added to a final concentration of 25 mM. The mixtures were incubated at 80℃ for 1 h to release the sialic acids from the samples. After centrifugation, the supernatant was collected, and added an equal volume of DMB (1,2-diamino 4,5-methylenedioxybenzene, Sigma-Aldrich, Inc.) solution containing 1.6 mg DMB in 1 mL of 1.4 M acetic acid, 0.75 M 2-mercaptoethanol and 18 mM $NaHSO_4$ and then incubated at 80℃ for 2 h to label the sialic acids. Neu5Gc and Neu5Ac (Sigma-Aldrich, catalog number: 50644 and A2388) were used as standard samples and were prepared by using a 1 mg/mL solution of each and labeling them identically under the same conditions. The DMB-labeled sample was injected onto a Waters™ HPLC system (Waters 2475 Multiwavelength Fluorescence Detector, Waters 717 plus Autosampler and Waters 600 Controller) with a Discovery® BIO wide Pore C18 (5 µm, 4.6 × 25 cm) column. The analysis was performed with an isocratic mobile phase of methanol: acetonitrile:H_2O ratio of 7:9:84 with a flow rate of 0.6 mL/min, and the

fluorescence detector was set at an excitation wavelength of 373 nm and an emission wavelength of 448 nm.

Histology of the SIS-ECM

All samples were fixed in 10% formalin solution for 24 h prior to staining with hematoxylin and eosin (H&E). The fixed samples were embedded in paraffin and sectioned for staining, and representative images were captured with an upright microscope (Nikon Eclipse E600).

Experiment Design and Intramuscular Implantation of the SIS-ECM

Growing pigs of 15~20 kg body weight, were used for this study. Atropine (0.1 mL /kg) and 0.5 mg Strenil (Janssen Pharm., Belgium) were injected intramuscularly. Animals were then anesthetized with an intramuscular injection of 2.0-8.8 mg/kg of Zoletil (Virbac S. A, FRA).

Under sterile conditions, the SIS-ECM (2 × 2 cm) prepared from the WT, CMAH KO ($_{CMAH}$KO) and the dual (GGTA1/CMAH) KO (dKO) pigs were individually implanted into the longissimus of WT and dKO pigs. A full-thickness skin incision of 3×3 cm in an “L” shape was created, and the deep fascia was opened. Then, the SIS-ECM was implanted into the longissimus and fixed with size 5-0 nylon sutures. The wound was closed with size 5-0 nylon sutures.

For the pathology analysis, six implants were implanted into each pig (WT and dKO) with three SIS-ECM implants from the dKO pigs on the right side and three SIS-ECM implants from the WT pigs on the left side.

After the indicated number of days, all animals were euthanized and exsanguinated. The tissues surrounding the implanted SIS-EMC were cut from the muscle and placed in 10% neutral buffered formalin.

To evaluate the effect of the serum IL-6 levels, three SIS-ECM implants from the same pigs were implanted into WT, $_{CMAH}$KO or dKO pigs into the same side of the back of each pig by the same procedure described above. Blood samples were collected from pigs on the indicated day for serum IL-6 measurement.

Pathology analysis

The tissues surrounding each test device were also preserved in 10% formalin for histopathological examination. The tissues were trimmed as necessary and embedded in paraffin. One section approximately 4 μm thick was prepared from each site. The slides were stained with hematoxylin and eosin (H&E) and assessed by light microscopy. The histologic evaluation index included multinuclear giant cells (MGC), inflammatory cell infiltration, granuloma formation, and neovascularization. The histopathologic grading of the local lesion response was based on the (4-point) scoring system presented

by Shackelford [16]: grade 0, within normal limits; grade 1, minimal; grade 2, slight; grade 3, moderate; and grade 4, severe.

Determination of IL-6 concentration

All blood samples were remained at 4°C and allowed to clot. After centrifugation at 1500×g, the serum samples were collected and stored at -20°C until analyzed. The concentration of IL-6 was determined in duplicate using a Swine IL-6 Pig ELISA kit (REF:ESIL6) from Thermo Fisher Scientific (Maryland, USA). All assays were performed according to the manufacturer's protocols. The detection limit of the kit was 45 pg/mL.

Results

Preparation of the SIS-EMC

The efficacy of the decellularization was evaluated by histological observation and the DNA content. Histological staining with H&E revealed the presences of visible and distinct nuclei in the small intestinal submucosa before (Figure 1A) and after (Figure 1B) removal of the inner mucosal layer and smooth muscle layers by mechanical disassociation. The nuclei could not be found in the samples after SDS treatment (Figure 1C).

The results from the DNA quantification showed that the SDS treatment produced a level of residual DNA in the SIS-EMC that is acceptable for medical devices. The DNA content differed in different animal sources, but the mechanical disassociation samples had a consistent value, approximately 110 ng DNA/mg SIS-ECM in the different samples of the SIS-EMC preparation. The extent of the DNA cleavage by the SDS treatment was more than 73% (Table 1). The DNA content levels were not significantly different than those obtained by the peracetic acid sterilization procedure. The purified DNA was tested by nested PCR for the DAP12 gene, and no DNA fragment of more than 200 bp could be observed for either the PCR or the nest-PCR amplicons (data not shown).

The SDS treatment did not significantly affect the glycosaminoglycan content of the SIS-EMC samples; and more than 90% glycosaminoglycan remained. However, the samples treated with peracetic acid showed a significant reduction of 66.2~68.4% in glycosaminoglycan content (Table 2). The amount of glycosaminoglycan and the ratio of its reduction during the SIS-EMC preparation process were similar to the values in the samples from 4- to 5-month-old pigs (Table 2). A small intestine sample from 13-month-old pigs was used to prepare the SIS-ECM, and the glycosaminoglycan content was 16.22±1.01, 15.05±0.45, and 10.56±0.47 μg/mg in the dKO (un), dKO (SDS) and dKO (All) samples, respectively, near to those from younger pigs.

Analysis of Neu5Gc and Neu5Ac

Tissues from the cornea, ear, tail and small intestine were analyzed. In WT pigs, both Neu5Ac and Neu5Gc were detected in the tissues, but only Neu5Ac could be found in the tissues from the $_{CMAH}$KO pigs. The content of Neu5Gc was less than that of Neu5Ac in the cornea, ear, and tail of WT pigs, but the Neu5Gc content was more than that of Neu5Ac in the small intestine of WT pigs (Figure 2A). According to the results of the HPLC analysis, no Neu5Gc was not found in the tissues from the $_{CMAH}$KO pigs. In this study, the process of decellularizing the WT SIS-EMC reduced the Neu5Gc content but obviously the Neu5Gc remained in the SIS-EMC (Figure 2B). Although Neu5Gc is a minor component in most tissues, including corneal (Figure 3C), none of the various decellularized processes could entirely remove it. Some processes, including treatment by N2 (showed in Figure 3D), SDS (showed in Figure 3E), formic acid, phospholipase and tonicity (data not show), were adapted to decellularize porcine cornea, but they all failed to remove Neu5Gc in the corneal products.

Pathology analysis

The findings from the various parameter evaluations of each lesion at different time courses (1-, 2- and 4-week) are summarized in Table 3. Multinuclear giant cell and inflammatory cell infiltration was evidently showed in 1-week in all groups. Granuloma formation was prominently observed in 4-week in all groups. Neovascularization was mostly exhibited in 4-week in all groups. Multinuclear giant cells were the least obvious in 4-week in the dKO (dKO) group and in 4-week in the WT (dKO) group. Inflammatory cell infiltration was the least noticeable in 4-week in the WT (dKO) and dKO (dKO) groups. Previous studies reported that the number of multinuclear giant cells (MGCs) and inflammatory cells can reflect the severity of the rejection reaction to implants [17]. According to the time course analysis, the numbers of MGCs and inflammatory cells (mainly lymphocytes) in the different groups were relatively low in the 4-week samples compared to those in the 1- and 2-week samples (Figure 4A). Interestingly, fewer MGCs were observed in the dKO (dKO) group than in the dKO (WT) group at 2-week. The pathological score of the MGCs of the dKO (WT) group (2.3±0.5) was significantly greater than that of the dKO (dKO) group (0.7±0.3) ($p<0.05$). The less severity of the lesions associated with MGCs was observed in the WT (dKO) group compared that of the lesions in the WT (WT) group but had no significantly difference to dKO (dKO) group at 4-week (Figure 4-I). Meanwhile, the inflammatory cells were minimally present in the WT (dKO) group compared with the number in the WT (WT) and dKO (WT) groups (Figure 4-II).

The indications of proliferation (granulation) were based on granuloma and neovascular formations (Table 3). The fibroblasts and endothelial cells were proliferating and maturing in the tissues with granulonma formation from weeks 2 to 4. The prominent vascularization of the granulomas indicated sufficient maintenance of a healing response. However, there were no significant differences in granuloma formation to indicate tissue maturation or blood vessel neovascularization among the groups. On the other hand, no evidence for chronic active inflammation or surrounding muscle necrosis was noted during the entire study period.

Changes in Serum IL-6 levels after SIS-ECM implantation

Except on day 7, the serum IL-6 concentrations were remained unchanged in all samples (Figure 5). A significant increase in serum IL-6 concentration was found in dKO (WT), $_{CMAH}$KO (WT) and dKO ($_{CMAH}$KO) samples on day 7, but the dKO (dKO) group had a lower serum IL-6 concentration on day 7 (Figure 5). The serum IL-6 concentrations of the dKO (dKO), dKO (WT), $_{CMAH}$KO (WT) and dKO ($_{CMAH}$KO) samples were 94.0±7.8, 424.5±26.5, 265 and 257.0 ng/mL, respectively. These results inferred that the Neu5Gc and α-Gal antigens caused the IL-6 production in the dKO pigs, as it would happen in human beings if implanted with scaffolds from WT pigs.

Discussion

In previous reports, the α-Gal epitope is persistently present within the ECM derived from the tissue of porcine origin despite a vigorous decellularization process [18-20]. In this study, Neu5Gc was also detected in the WT pig SIS-ECM that was produced by the decellularization process. For comparison, several commercial ECM products were analyzed, and Neu5Gc was detected in all the products (data not shown) proving our dKO SIS-ECM is novel with biocompatibility.

During evolution, the human CMAH gene was mutated and does not express intrinsic Neu5Gc; however, human serum contains anti-Neu5Gc antibodies, which represents the majority of the non-Gal antibodies that limit xenotransplantation [21,22]. Similar to Neu5Gc, α-Gal cannot be synthesized by humans due to a loss-of-function mutation in the GGTA1 gene, but all humans carry anti-α-Gal antibodies. It is worth noting that α-Gal has a single carbohydrate xenogeneic antigen (Galα1-3–Galβ1-4–GlcNAc-R) [23], but there are multiple Neu5Gc-glycans on glycoproteins and glycolipids. These findings agreed with the report that the complexity of Neu5Gc should be seriously considered in xenotransplantation [11]. Our results showed that acellular SIS-ECM allografts implanted into dKO when compared to WT or pigs caused lower histopathologic scores of the lesions and unchanged serum IL-6 concentration, indicated no serious immune response. A previous study demonstrated that porcine-derived scaffold containing the α-Gal epitope induced a serum antibody response, but this α-Gal epitope had no adverse effects on the host remodeling response [24]. A recent article reported that, in a nonhuman primate model, decellularized WT and α-Gal KO porcine lung scaffold implants differed little in terms of immunological responses, although the latter showed delayed immune cell infiltration and downregulated chronic T-cell-mediated reactions to the scaffold [25].

During wound healing, platelets release factors throughout the formation of the hemostatic wound plug and initiate the inflammatory response [26]. This inflammatory response is, in part, mediated by proinflammatory cytokines, such as IL-6, which are produced by fibroblasts and macrophages in response to the factors released in the hemostatic wound plug [27]. These proinflammatory cytokines recruit inflammatory cells, including polymorphonuclear cells, monocytes, and macrophages, into the wound. The inflammatory cells are then activated and produce more inflammatory cytokines, causing additional inflammation and cytokine production. These inflammatory cells also produce growth factors that stimulate both fibroblast proliferation and modify the ECM, leading to scar formation [28], which exerted an important effect in the remodeling response [29]. A study on the implantation of non-cross-

linked acellular matrices (scaffold) showed that IL-6 positive cells were increased at day 14 and successively decreased thereafter [30]. This IL-6 expression was observed in the location surrounding the wound site in the wound-healing experiments [30]. During transplantation, the serum level of IL-6 increases in association with inflammatory reactions, including allograft rejection [31-33]. Furthermore, IL-6 has been investigated extensively in clinical transplant patients since a relatively large amount of IL-6 is released during the early phase of immune activation [34,35]. Blocking both TNF-α and IL-6 was, therefore, beneficial in a pig-to-baboon kidney xenotransplant and that a blockade of two or even more cytokines together could further reduce xenograft rejection [36].

In this study, there was no obvious increase in IL-6 levels in the serum of all the experimental animals 2 days after SIS-ECM implantation. The lower levels of serum IL-6 on day 2 may result from the acellular matrix implanted into the muscles of pigs and caused no infection in the surgical wounds. The serum IL-6 level was increased on day 7 and then decreased to a level comparable to that before implantation (Figure 5). These data agreed with the histological analysis of the tissues near the implanted SIS-ECM. In our results, the SIS-ECM from the WT and KO pigs were implanted into the muscles of the pigs, and the tissues were examined after 1-, 2-, and 4-week (Table 3). The results from the histopathologic analysis revealed that the tissues surrounding the SIS-ECM exhibited a prominent host tissue response, with areas of dense accumulation of inflammatory cells along with multinucleated giant cells at 1-week, and the cell infiltration gradually decreased by 2- and 4-week. The novel finding was that different IL-6 levels were detected in the sera from different experimental groups. The Neu5Gc content in the SIS-ECM from the WT pigs was analyzed by HPLC, and a considerable amount of Neu5Gc was detected. The presence of the α-Gal epitope in biologic scaffolds has been investigated for porcine SIS-ECM [37]. In this study, Neu5Gc and α-Gal were xeno-antigens from the WT or the KO pigs, as their SIS-EMC were implanted into the dKO pigs, the WT SIS-EMC was implanted into the $_{CMAH}$KO pigs, and the $_{CMAH}$KO SIS-EMC was implanted into dKO pigs. Each group of recipient animals increased their serum IL-6 levels. In contrast, in the group of dKO pigs which the dKO SIS-EMC were implanted, the serum IL-6 level changed little. A previous report [30] on the biocompatibility of porcine skin scaffolds, as assessed 3, 14, 21 and 90 days after their implantation in rats, indicated that the implants were surrounded by polymorphonuclear cells on day 3 and then were replaced by a notable number of IL-6 positive cells by day 14. The time course of cell infiltration, IL-6 expression, and tissue remodeling were all delayed in comparison with the responses shown by the data of our study. The discrepancy may result from the difference of animal used (rats versus pigs) and the implant site selected (subcutaneous tissue versus muscle).

Macrophages are one of the broadest ranging cell types capable of polarizing entirely from being contributors to tissue inflammation (M1 macrophage) toward being contributors to wound healing (M2 macrophage) [38]. Classical M1 macrophages are induced in response to lipopolysaccharide-expressing pro-inflammatory cytokines such as TNFα, IL-6, and IL-1β, of which all contribute to tissue inflammation and osteoclastogenesis. The M2 macrophages are induced by IL-4 and IL-13 and typically produce TGF-β and arginase, both of which are implicated in the tissue repair process. Histopathologically, the role of multinucleated giant cells around certain classes of biomaterials has been directly linked to xeno-

rejection, but a recent article suggested that it is necessary to better characterize them scientifically and appropriately as M1-MGC and M2-MGC accordingly [39].

Obtained results clearly suggested that SIS-ECM derived from dKO pigs showed little antigenic response to α-Gal or N-glycolylneuraminic acid, as determined by the histopathologic scores of the local response lesions and serum IL-6 concentration in the implanted dKO pigs. Those animals can not only serve as biocompatible SIS-ECM donors but also be used as animal models for testing anthropomorphic immune responses to biomedical devices.

Conclusions

The SIS-ECM derived from dKO pigs showed little antigenic response to α-Gal or N-glycolylneuraminic acid and therefore has observed lower inflammatory response in the implanted pigs. We have shown that the acellularized SIS-ECM derived from KO pigs performed superior and present a promising future of clinical application. A novel animal model for antigenic response to α-Gal or N-glycolylneuraminic acid has also established.

References

1. Prevel CD, Eppley BL, Summerlin DJ, Sidner R, Jackson JR, McCarty M, et al. Small intestinal submucosa: utilization as a wound dressing in full-thickness rodent wounds. Ann. Plast. Surg. 1995;35:381-8.
2. Lam MT, Nauta, A, Meyer NP, Wu JC, Longaker MT. Effective delivery of stem cells using an extracellular matrix patch results in increased cell survival and proliferation and reduced scarring in skin wound healing. Tissue Eng. Part A. 2013;19:738-47.
3. Niezgoda JA, Van Gils CC, Frykberg RG, Hodde JP. Randomized clinical trial comparing OASIS Wound Matrix to Regranex Gel for diabetic ulcers. Adv. Skin Wound Care. 2005;18:258-66.
4. Mostow, E.N., Haraway, G.D., Dalsing, M., Hodde, J.P., King, D., OASIS Venus Ulcer Study Group. Effectiveness of an extracellular matrix graft (OASIS Wound Matrix) in the treatment of chronic leg ulcers: a randomized clinical trial. J. Vas. Surg. 2005; 41:837-43.
5. Badylak SF, Freytes DO, Gilbert TW. Extracellular matrix as a biological scaffold material: Structure and function. Acta Biomater. 2009;5:1-13.
6. Shi L, Ronfard V. Biochemical and biomechanical characterization of porcine small intestinal submucosa (SIS): a mini review. Int. J. Burns Trauma, 2013;3:173-9.
7. Zheng MH, Chen J, Kirilak Y, Willers C, Xu J, Wood D. Porcine small intestine submucosa (SIS) is not an acellular collagenous matrix and contains porcine DNA: possible implications in human implantation. J. Biomed. Mater. Res. B Appl. Biomater. 2005;73:61-7.
8. Badylak SF, Gilbert TW. Immune response to biologic scaffold materials. Semin. Immunol. 2008;20:109-16.

9. Bornhöfft KF, Goldammer T, Rebl A, Galuska SP. Siglecs: A journey through the evolution of sialic acid-binding immunoglobulin-type lectins. Dev. Comp. Immunol. 2018;86:219-31.
10. Altman MO, Gagneux P. Absence of Neu5Gc and presence of anti-Neu5Gc antibodies in humans—an evolutionary perspective. Front Immunol. 2019;10:789.
11. Paul A, Padler-Karavani V. Evolution of sialic acids: Implications in xenotransplant biology. Xenotransplantation 2018;6:e12424.
12. Chuang C-K, Chen C-H, Huang C-L, Lin Y-J, Su Y.-H, Peng S-H, et al. Generation of GGTA1 mutant pigs by direct pronuclear microinjection of CRISPR/Cas9 plasmid vectors. Anim. Biotechnol. 2017;28:174-81
13. Tu C-F, Chuang C-K, Hsiao K-H, Chen C-H, Chen C-M, Peng S-H, et al. Lessening of porcine epidemic diarrhoea virus susceptibility in piglets after editing of the CMP-N-glycolylneuraminic acid hydroxylase gene with CRISPR/Cas9 to nullify N-glycolylneuraminic acid expression. Plos one 2019;14:e0217236.
14. Badylak SF, Lantz GC, Coffey A, Geddes LA. Small intestinal submucosa as a large diameter vascular graft in the dog. J. Surg. Res. 1989;47:74-80.
15. Syed O, Walters NJ, Day RM, Kim HW, Knowles JC. Evaluation of decellularization protocols for production of tubular small intestine submucosa scaffolds for use in oesophageal tissue engineering. Acta Biomater. 2014;10:5043-54.
16. Shackelford C, Long G, Wolf J, Okerberg C, Herbert R. Qualitative and quantitative analysis of nonneoplastic lesions in toxicology studies. Toxicol. Pathol. 2002;30:93-6.
17. Sheikh Z, Brooks PJ, Barzilay O, Fine N, Glogauer M. Macrophages, Foreign Body Giant Cells and Their Response to Implantable Biomaterials. Materials 2015; 8:5671-701.
18. McPherson TB, Liang H, Record RD, Badylak SF. Galα(1,3)Gal epitope in porcine small intestinal submucosa. Tissue Eng. 2000;6:233-9.
19. Kasimir MT, Rieder E, Seebacher G, Nigisch A, Dekan B, Wolner E, et al. Decellularization does not eliminate thrombogenicity and inflammatory stimulation in tissue-engineered porcine heart valves. J. Heart Valve Dis. 2006;15:278-86.
20. Kasimir MT, Rieder E, Seebacher G, Wolner E, Weigel G, Simon P. Presence and elimination of the xenoantigen gal (alpha1, 3) gal in tissue-engineered heart valves. Tissue Eng. 2005;11:1274-80.
21. Padler-Karavani V, Yu H, Cao H, Chokhawala H, Karp F, Varki N, et al. Diversity in specificity, abundance, and composition of anti-Neu5Gc antibodies in normal humans: potential implications for disease. Glycobiology 2008;18:818-30.
22. Zhu A, Hurst R. Anti-N-glycolylneuraminic acid antibodies identified in healthy human serum. Xenotransplantation 2002;9:376-81.
23. Galili U. The alpha-gal epitope and the anti-Gal antibody in xenotransplantation and in cancer immunotherapy. Immunol. Cell Biol. 2005;83:674-86.

24. Daly KA, Stewart-Akers AM, Hara H, Ezzelarab M, Long C, Cordero K, et al. Effect of the alphaGal epitope on the response to small intestinal submucosa extracellular matrix in a nonhuman primate model. Tissue Eng. Part A 2009;15: 3877-88.
25. Stahl EC, Bonvillain RW, Skillen CD, Burger BL, Hara H, Lee W, et al. Evaluation of the host immune response to decellularized lung scaffolds derived from a-Gal knockout pigs in a non-human primate model. Biomaterials 2018;187:93-104.
26. Moulin V. Growth factors in skin wound healing. Eur. J. Cell Biol. 1995;68:1-7.
27. Shabo Y, Lotem J, Sachs L. Autoregulation of interleukin 6 and granulocyte-macrophage colonystimulating factor in the differentiation of myeloid leukemic cells. Mol. Cell Biol. 1989;9:4109-12.
28. Roth M, Nauck M, Tamm M, Perruchoud AP, Ziesche R, Block LH. Intracellular interleukin 6 mediates platelet-derived growth factor-induced proliferation of nontransformed cells. Proc. Natl. Acad. Sci. USA 1995;92:1312-6.
29. Barrientos S, Stojadinovic O, Golinko MS, Brem H, Tomic-Canic M. Growth factors and cytokines in wound healing. Wound Repair Regen. 2008;16:585-601.
30. Mimura KK, Moraes AR, Miranda AC, Greco R, Ansari T, Sibbons P, et al. Mechanisms underlying heterologous skin scaffold-mediated tissue remodeling. Sci. Rep. 2016;6:35074.
31. Kita Y, Iwaki Y, Demetris AJ, Starzl TE. Evaluation of sequential serum interleukin-6 levels in liver allograft recipients. Transplantation 1994;57:1037-41.
32. Van Oers MHJ, Van Der Heyden AAPAM, Aarden LA. Interleukin 6 (IL-6) in serum and urine of renal transplant recipients. Clin. Exp. Immunol. 1988;71:314-9.
33. Matsumiya G, Gundry SR, Nehlsen-Cannarella S, Fagoaga OR, Morimoto T, Arai S, et al. Serum interleukin-6 level after cardiac xenotransplantation in primates. Transplant Proc 1997;29:916-9.
34. Schwaighofer H, Herold M, Schwarz T, Nordberg J, Ceska M, Prior C, et al. Serum levels of interleukin 6, interleukin 8, and C-reactive protein after human allogeneic bone marrow transplantation. Transplantation 1994;58:430-6.
35. Fyfe A, Daly P, Galligan L, Pirc L, Feindel C, Cardella C. Coronary sinus sampling of cytokines after heart transplantation: evidence for macrophage activation and interleukin-4 production within the graft. J. Am. Coll. Cardiol. 1993;21:171-6.
36. Zhao Y, Cooper DKC, Wang H, Chen P, He C, Cai Z, et al. Potential pathological role of pro-inflammatory cytokines (IL-6, TNF-α, and IL-17) in xenotransplantation. Xenotransplantation 2019;16:e12502.
37. McPherson TB, Liang H, Record RD, Badylak SF. Galα(1,3)Gal epitope in porcine small intestinal submucosa. Tissue Eng. 2000;6:233-9.
38. Martinez FO, Gordon S. The M1 and M2 paradigm of macrophage activation: time for reassessment. F1000Prime Rep. 2014;6:13.

39. Miron RJ, Bosshardt DD. Multinucleated Giant Cells: Good Guys or Bad Guys? Tissue Eng. Part B Rev. 2018;24:53-65.

Declarations

Ethics approval and consent to participate

Permission to undertake the SIS implantation experiments was granted by the institution (IACUC Approval Nos. 105129 and 107060, Agriculture Technology Research Institute) where the animal study was conducted.

Consent for publication

Not applicable.

Availability of data and materials

Please contact author for the requests.

Competing interests

There are no conflicts to declare.

Funding

This study was financially supported by the Council of Agriculture, Executive Yuan, Taiwan ROC, through the projects of 105AS-6.3.4-AD-U1, 106AS-6.3.2-AD-U1, 105AS-6.2.1-ST-a1 and 106AS-6.2.1-ST-a1.

Authors' contributions

Performed the experiment and the analysis: Chon-Ho Yen, Hao-Chih Tai, Ching-Fu Tu, and Su-Hei Peng. Wrote the Manuscript: Chon-Ho Yen, Tien-Shuh Yang, and Ching-Fu Tu. Design the experiment: Chon-Ho Yen, Hao-Chih Tai, and Ching-Fu Tu. All authors read and approved the final manuscript.

Acknowledgements

This study was financially supported by the Council of Agriculture, Executive Yuan, Taiwan ROC, through the projects of 105AS-6.3.4-AD-U1, 106AS-6.3.2-AD-U1, 105AS-6.2.1-ST-a1 and 106AS-6.2.1-ST-a1. Thanks are also due to Mrs. K.-X. Hsiao, C.-Y. Hsu, and C.-H. Wong, and Ms M.-S. Leu for their animal care and/or technical services, and to Drs. Y.-F. Wu and T.-Y. Xiang for their assistance in animal experiment.

Tables

Table 1. The clearance efficiency of SDS on DNA content in porcine SIS-ECM.

Sample	DNA, ng/mg	DNA reducing, %
WT-u	434.7 ±13.0	73.6
WT-t	114.9 ±11.6	
$_{CAMH}$KO-u	609.3±17.3	83.2
$_{CAMH}$KO-t	102.2±2.1	
dKO-u	442.0±27.3	74.7
dKO-t	112.0±15.8	

The reduction of DNA content by SDS treatment was analyzed for three lots of porcine SIS-ECM preparations. WT, dKO and CAMHKO represent the small intestines from the wild-type, the GATT1/CAMH double KO and the CAMH KO pigs, respectively. “XX-u” and “XX-t” indicate the samples before and after SDS treatment. Data are expressed as the mean ± SEM (n=3) .

Table 2. Glycosaminoglycan content of the samples during the process for producing SIS-ECM.

Samples	GAG content, µg/mg of SIS	GAG ratio, % (treated/untreated)
WT (un)	14.73±0.46	100.0
WT (SDS)	13.69±0.29	92.9
WT (All)	10.08±0.40	68.4
$_{CMAH}$KO (un)	15.26±0.36	100.0
$_{CMAH}$KO (SDS)	14.32±0.37	93.8
$_{CMAH}$KO (All)	10.21±0.41	66.9
dKO (un)	14.95±0.35	100.0
dKO (SDS)	14.05±0.48	94.0
dKO (All)	9.89±0.36	66.2

Note: WT, dKO and $_{CAMH}$KO represent the small intestines from wild-type, the GATT1/CAMH double KO and the CAMH KO pigs, respectively. (un)= treated with mechanical abrasion; (SDS) = after SDS treatment; and (All)= after peracetic acid treatment. Data are expressed as the mean ± SEM (n=3).

Table 3. Histopathological findings of implanted materials.

Specimens		Multinuclear giant cells	Inflammatory cells infiltration	Granuloma formation	Neo-vascularization
1-w	WT(WT)	4.0±0.0	4.0±0.0	1.0±0.0	1.0±0.0
	WT(dKO)	4.0±0.0	4.0±0.0	1.3±0.3	1.0±0.0
	dKO(WT)	4.0±0.0	4.0±0.0	1.0±0.0	1.0±0.0
	dKO (dKO)	3.7±0.3	4.0±0.0	1.0±0.0	1.0±0.0
2-w	WT(WT)	1.7±0.5	2.0±0.5	1.7±0.3	3.7±0.3
	WT(dKO)	2.0±0.5	1.7±0.3	2.0±0.0	4.0±0.0
	dKO(WT)	2.3±0.5*	2.7±0.3	2.0±0.0	4.0±0.0
	dKO(dKO)	0.7±0.3*	2.3±0.3	2.0±0.0	4.0±0.0
4-w	WT(WT)	1.7±0.5	2.0±0.5	3.0±0.0	2.0±0.5
	WT(dKO)	0.3±0.3	0.7±0.3	3.0±0.0	2.3±0.3
	dKO(WT)	1.0±0.5	1.7±0.3	3.0±0.0	2.7±0.3
	dKO(dKO)	0.7±0.3	1.3±0.3	3.0±0.0	2.7±0.3

Note: w= week; *p<0.05. The result shows the histopathological findings for the materials implanted into wild-type pigs and GATT1 and CAMH double KO pigs at the indicated implantation time. The final numerical score was calculated by dividing the sum of the number of affected samples per grade by the total number of examined specimens. The data are expressed as the mean ± SEM for three specimens in the experiment. In the parentheses indicate SIS-ECM from the wild-type or the dKO pigs. For example, dKO (WT) represents the SIS-ECM from the wild-type pigs implanted into the dKO pigs. The histopathological scores were graded 0-4 as follows: Grade 0, within normal limits; Grade 1, minimal; Grade 2, slight; Grade 3, moderate; and Grade 4, severe. * Statistically significant difference between the control and treated groups at p<0.05.

Figures

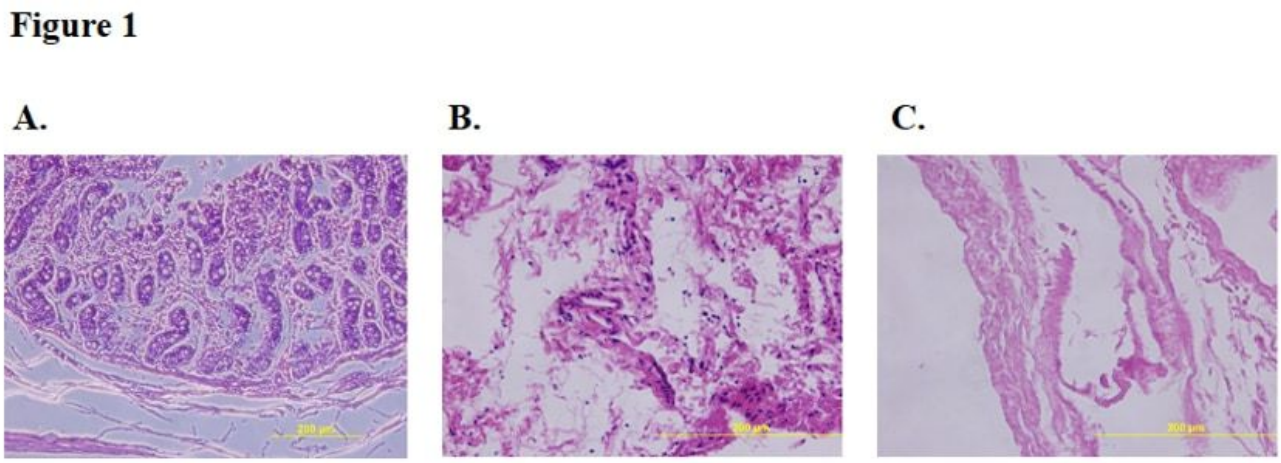

Figure 1

Histological images of the decellularized SIS-ECM and the controls. A. untreated small intestine; B. small intestine after mechanical disassociation; C. small intestine after SDS treatment.

Figure 2

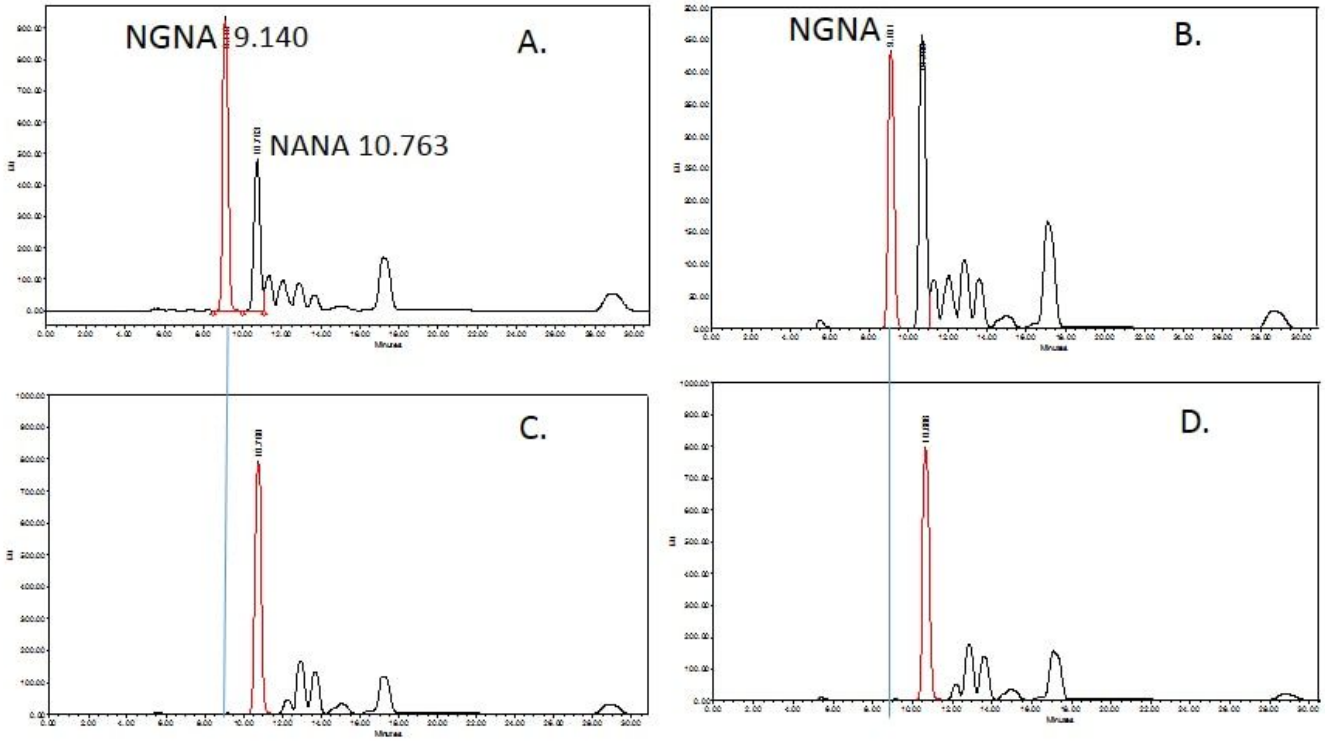

Figure 2

The HPLC analysis of Neu5Gc (NGNA) and Neu5Ac (NANA) in porcine small intestine submucosa before and after decellularization. Panel A shows the results from an analysis of wild-type (WT) porcine small intestine submucosa before decellularization. Panel B shows the WT porcine small intestine submucosa after decellularization. Panel C shows the Neu5Gc levels in the α-Gal and CAMH double KO (dKO) porcine small intestine submucosa before decellularization. Panel D shows the dKO porcine small intestine submucosa after decellularization. The retention times of Neu5Gc and Neu5Ac are indicated in the figure.

Figure 3

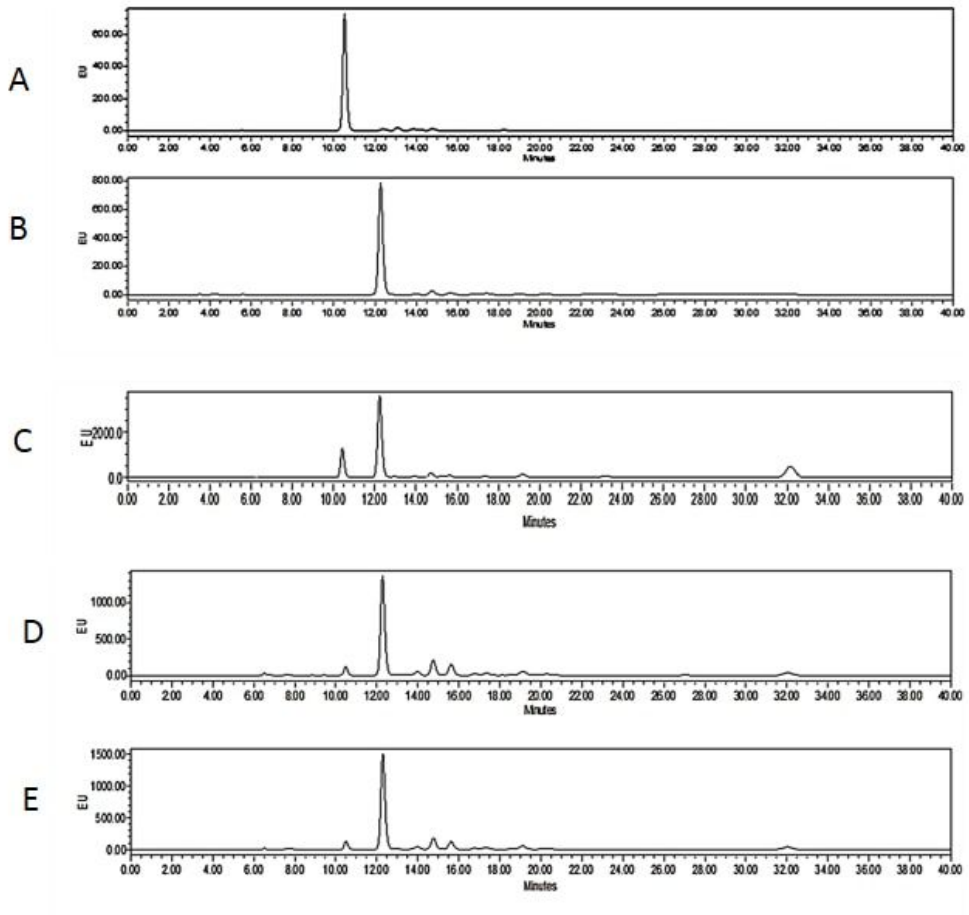

Figure 3

The HPLC analysis of Neu5Gc and Neu5Ac in porcine cornea before and after decellularization. Panel A and B shows the Neu5Gc and NEU5AC standard, respectively. Panel C shows the cornea of wild-type porcine before decellularization. Panel D shows the cornea of wild-type porcine after decellularization as determined with the liquid N2 vapour method. Panel E shows the cornea of the wild-type porcine after decellularization with SDS.

Figure 4

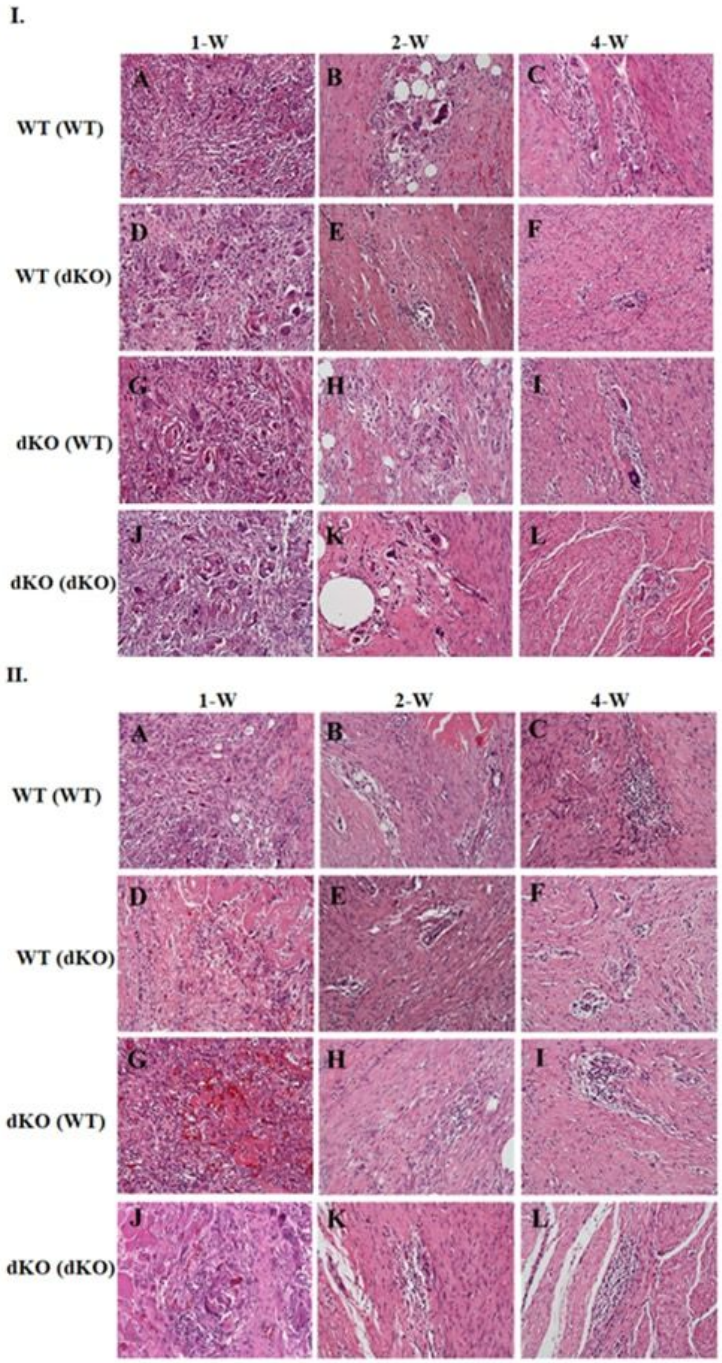

Figure 4

Histopathological examination of tissue biocompatibility in the implantation study. Representative sections of the implantation sites at 1, 2, and 4 weeks post implantation. WT (WT) group (A, B, C), WT (dKO) group (D, E, F, dKO (WT) group (G, H, I), dKO (dKO) group (J, K, L). Panels (I) and (II) show the pathological score as assessed for the multinuclear giant cells and inflammatory cells, respectively. Multinuclear giant cell and inflammatory cell infiltration was most obvious in the first week in all groups.

Granuloma formation was most obvious in the fourth week in all groups. Neovascularization was most obvious in the third week in all groups. Multinuclear giant cells were less obvious in the second week in the dKO (dKO) group. The inflammatory cell infiltration was less obvious in the second week in the WT (dKO) and dKO (dKO) groups. The slices were assessed by light microscopy (200×).

Figure 5

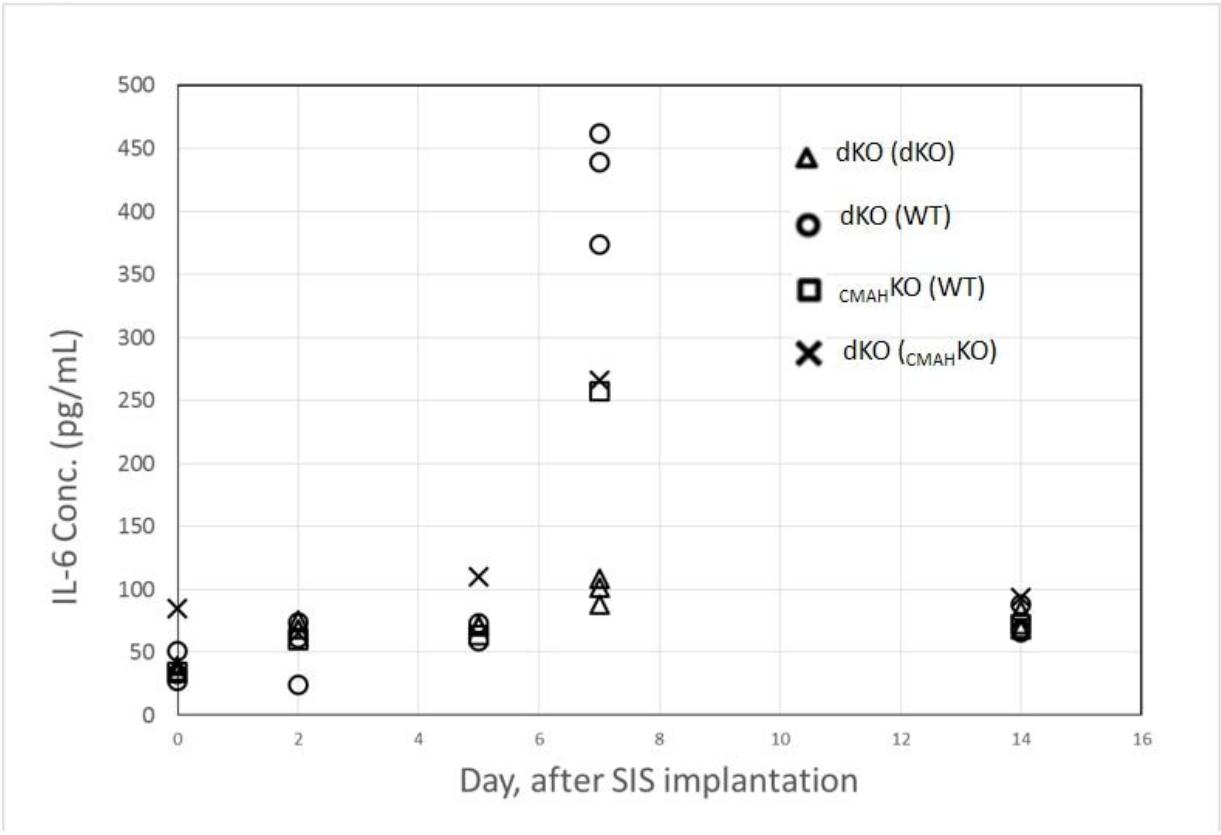

Figure 5

Serum concentrations of IL-6 in pigs implanted with SIS-ECM. dKO (dKO) represents the SIS-ECM from the double GGTA1 and CMAH KO pigs implanted into the dKO pigs (n=3). dKO (WT) represents the SIS-ECM from the wild-type (WT) pigs implanted into the dKO pigs (n=3). CMAHKO (WT) represents SIS-ECM from the WT. pigs implanted into the CMAHKO pigs (n=1). dKO (CMAHKO) represents the SIS-ECM from the CMAH KO pigs implanted into the dKO pigs (n=1).